

# Non-variable cosmologically distant gamma-ray emitters as an imprint of propagation of ultra-high-energy protons

A.Yu. Prosekin<sup>1</sup>, S.R. Kelner<sup>1</sup>, and F.A. Aharonian<sup>1,2</sup>

<sup>1</sup> Max-Planck-Institut für Kernphysik, Saupfercheckweg 1, D-69117 Heidelberg, Germany  
e-mail: Anton.Prosekin@mpi-hd.mpg.de

<sup>2</sup> Dublin Institute for Advanced Studies, 31 Fitzwilliam Place, Dublin 2, Ireland

January 15, 2012

## ABSTRACT

The acceleration sites of ultra-high-energy (UHE) protons can be traced by the footprint left by these particles propagating through cosmic microwave background (CMB) radiation. Secondary electrons produced in extended region of several tens of Mpc emit their energy via synchrotron radiation predominantly in the initial direction of the parent protons. It forms a non-variable and compact (almost point-like) source of high energy gamma rays. The importance of this effect is increased for cosmologically distant objects; because of severe energy losses, UHE protons cannot achieve us even in the case of extremely weak intergalactic magnetic fields. Moreover, at high redshifts the energy conversion from protons to secondary particles becomes significantly more effective due to the denser and more energetic CMB in the past. This increases the chances of UHE cosmic rays to be traced by the secondary synchrotron gamma radiation. We discuss the energy budget and the redshift dependence of the efficiency of energy transfer from UHE protons to synchrotron radiation. The angular and spectral distributions of radiation in the gamma- and X-ray energy bands are calculated and discussed in the context of their detectability by *Fermi LAT* and *Chandra* observatories.

**Key words.** ultrahigh energy cosmic rays – gamma-ray emission – X-ray emission – point-like source – high redshift – propagation

## 1. Introduction

Although there is a little doubt that UHE cosmic rays,  $E \geq 10^{19}$ eV, are produced in extragalactic sources, the nature and origin of these objects remain highly unknown. In the case of very weak intergalactic magnetic fields (IGMF), the initial directions of these particles is only moderately entangled, and thus the information about their acceleration sites can be partly preserved. The quantitative treatment of propagation of UHE cosmic rays is limited because of large (orders of magnitude) uncertainties of relevant model parameters. Especially it concerns the IGMF. The current measurements give only upper limit  $B \sim 10^{-9}$  G for the component parallel to the line of sight (Ryu et al. 1998; Blasi & Olinto 1999); the lower bound is estimated as small as of  $B \sim 10^{-16}$  G (see Taylor et al. (2011) and references therein) from the non-observations of GeV gamma-ray counterparts from distant TeV blazars. The large scale structure of IGMF is also very uncertain; the attempts to model usually lead to quite different results (Dolag et al. 2005; Sigl et al. 2004). These uncertainties significantly limit the potential of the so-called cosmic ray astronomy. Moreover, even in the case of very weak magnetic fields, the cosmic ray "horizon" of UHE cosmic ray sources through direct detection of these particles is limited by interactions with CMBR. For highest energy particles,  $E \sim 10^{20}$ eV, it does not exceed 100 Mpc. At lower energies cosmic rays can propagate to significantly larger distances, but they are dramatically deflected by galactic magnetic fields. These two factors significantly limit the potential of the so-called *proton astronomy*.

An important information about the acceleration sites of UHE protons is contained in gamma rays produced during propagation of protons through the CMBR. In the case of very low intergalactic magnetic field, the secondary products of *py* inter-

actions initiate electromagnetic cascades in CMBR. The effective development of such cascades is determined by the dominance of Compton energy losses over the synchrotron losses of secondary electrons. Generally, this condition is quite relaxed; it requires IGMF weaker than  $10^{-10}$ G. However, the second condition of detection of cascade gamma rays in the direction of parent UHE protons requires much weaker magnetic fields, smaller than  $10^{-15}$ G. Otherwise the relatively low energy electrons, and consequently the GeV and TeV gamma-ray emission, will be immediately isotropised. Formally, such weak intergalactic magnetic fields cannot be excluded. Moreover, recently it has been argued that very high energy tails of gamma-ray spectra of distant TeV blazars might be contributed by cascades initiated by UHE protons in intergalactic medium with magnetic field as small as  $10^{-15}$ G (Essey et al. 2011).

Remarkably, even in the case of strong IGMF, we might expect physically extended (but looking point-like) gamma-ray sources formed around production sites of UHE cosmic rays (Gabici & Aharonian 2005; Aharonian et al. 2010; Kotera et al. 2011). In this case gamma rays are produced through synchrotron radiation of secondary electrons from photomeson interactions. Protons lose significant fraction of their energy on scales of several tens of Mpc. If the magnetic field in these regions located at relatively small redshifts,  $z \ll 1$ , are significantly large,  $B \geq 10^{-9}$ G (so the energy of secondary electrons is released in the gamma-ray band), but smaller than  $10^{-7}$ G (thus the initial directions of electrons are not dramatically changed), the resulting gamma-ray synchrotron sources can be quite compact with an angular size as small as  $0.1^\circ$ .

For cosmologically distant sources embedded in denser ( $n_{\text{ph}} \propto (1+z)^3$ ) and more energetic ( $T \propto 1+z$ ) CMBR, protons lose their energy on distances significantly smaller than

100 Mpc. In the presence of magnetic field of strength  $B = 10^{-9} - 10^{-8}$  G the high energy electrons produced in photomeson processes intensively emit synchrotron radiation in GeV range of energies. The electrons radiate most of their energy on almost rectilinear part of the path that gives, along with the small deflection of protons, collimated beam of gamma rays pointing to the acceleration site of UHE protons. Note that the considerable contribution to the high energy electrons is provided by the gamma rays produced in decay of mesons. The interaction of these gamma rays with cosmic radio background radiation occurs in the regime when the most of the energy goes to one of the component of the created electron-positron pair.

The probability of detection of cosmic ray sources via synchrotron radiation of secondary electrons strongly depends on the maximum energy of accelerated protons. In the case of sources with redshift  $z \ll 1$ , the interaction of protons with CMBR is effective only when the proton spectrum extends to  $10^{20}$  eV and beyond. Since acceleration of protons to such high energies can be realized only at a unique combination of a few principal parameters, in particular the linear size of the source, the strength of the magnetic field, and the Lorentz factor of the bulk motion (Aharonian et al. (2002)), the number of sources of  $10^{20}$  eV cosmic rays can be quite limited compared to sources accelerating particles to  $E_{\max} \sim 10^{19}$  eV. Since protons at high redshifts interact with denser and more energetic photons of CMBR, the requirement to  $E_{\max}$  is significantly relaxed, thus one should expect dramatic increase of the number of UHE cosmic ray sources surrounded by gamma-ray halos. Furthermore, at high redshifts the interaction of protons with CMBR via pair production (Berhe-Heitler) process begins to play an important role and a considerable part of proton energy is converted to less energetic electrons compared to electrons generated in photomeson reactions. Appearance of dense halos of Bethe-Heitler electrons around the source at presence of magnetic field of the order of  $B \sim 10^{-6}$  G (comparable to the field of clusters of galaxies) results in radiation dominated by synchrotron X-rays.

In this paper we study the energy and angular distribution of the synchrotron gamma-ray emission from cosmologically distant sources. The calculations are based on the approach developed in our previous work (Aharonian et al. (2010)) combined with cosmological effects on propagation of gamma rays and protons. The space in the vicinity of the source, where all relevant processes occur, can be considered as conventional one. Therefore, taking into account denser ambient radiation at high redshifts, we can apply the developed formalism to calculation of the distribution function of gamma rays in the vicinity of the source. Using this function, we can easily obtain the distribution function of the observed radiation which has propagated cosmological distance (see Appendix A).

## 2. Energy budget

An accelerator of UHE protons located at high redshift has appreciably different conditions of ambient media as compared to the ones in the nearby Universe. The photon field of CMB is denser and more energetic due to cosmological expansion. The increase of density by factor of  $(1+z)^3$  leads to more frequent interactions of UHE protons with CMB that intensifies the energy loss rate. The average energy of photons is also increased by factor of  $(1+z)$  that decreases the threshold energy of the interactions for protons. The energy loss rate of protons due to

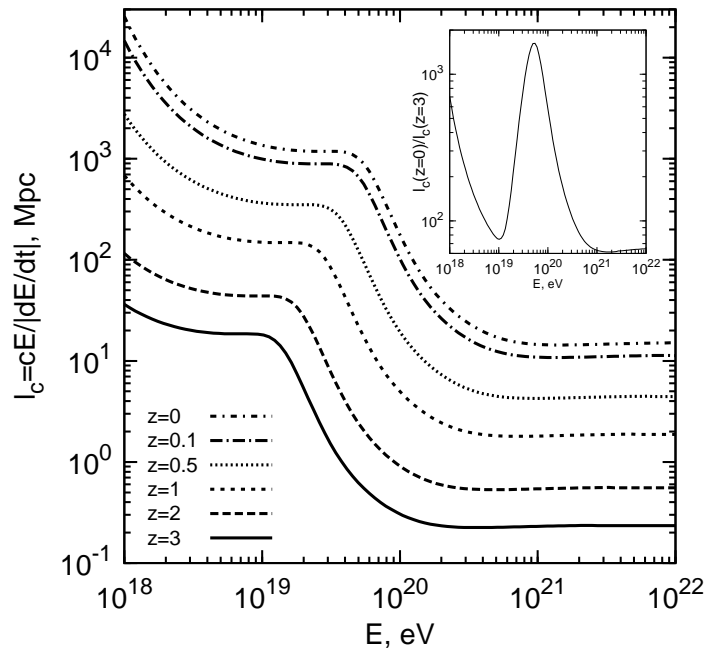


**Fig. 1.** The cooling length of protons in the intergalactic medium due to interactions with photons of CMBR at different redshift. The ratio of cooling lengths at  $z = 0$  and  $z = 3$  are shown in the inset.

interaction with CMB at the epoch of redshift  $z$  is expressed in terms of the present loss rate  $\beta(E) = -\frac{1}{E} \frac{dE}{dt}$  as

$$\beta(E, z) = (1+z)^3 \beta_0((1+z)E). \quad (1)$$

It is convenient to present this relation in terms of the cooling length which is shown in Fig. 1. The cubic dependence on redshift leads to considerable decrease of the cooling length. In particular, for the constant losses at highest energies,  $E \geq 10^{21}$  eV, it is reduced from  $\approx 15$  Mpc at the present epoch to  $\approx 0.2$  Mpc at  $z = 3$ . The plateau of constant losses itself extends to lower energies due to the energy shift. At lower energies, the combination of the effects related to the energy shift and the increase of density jointly results in reduction of cooling length by a factor larger than  $(1+z)^3$ . Indeed, as it is seen from the inset in Fig. 1 the reduction of the proton cooling length can be an order of magnitude larger. The peaks show domains where energy loss at  $z = 3$  is the most intensive relative to the case of present epoch. If the energy cutoff in the initial proton spectrum falls into this domain, the advantage of energy extraction at cosmological distances becomes more significant. Moreover, at  $E = 10^{18}$  eV, the cooling length is reduced from  $\geq 10^4$  Mpc at  $z = 0$  to tens of Mpc at  $z = 3$ . It is interesting to note that the energy loss rate of protons of energy  $E < 10^{19}$  eV at  $z = 3$  is comparable to the loss rate of  $E \geq 10^{20}$  eV protons at the present epoch.

Fig. 2 describes the evolution of proton energy losses and the efficiency of their conversion to the electron component of secondaries with the distance to the source at different redshifts. The electron component includes the electrons produced through all channels under consideration: pair production by protons, decay of charged mesons produced in photomeson processes and pair production by gamma rays produced from decay of neutral mesons. As mentioned above, in the latter process almost all energy of the photon goes to the energy of one of the electrons. Therefore the gamma rays can be treated as electrons.

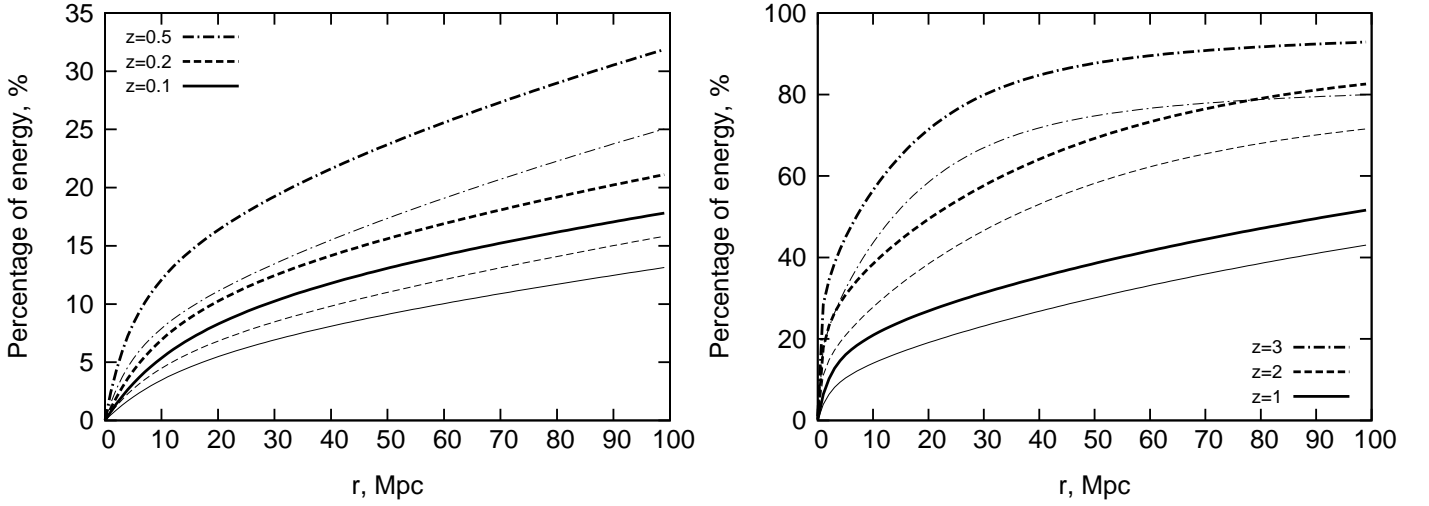


**Fig. 2.** The fraction of the initial energy of protons with  $E > 10^{18}$  eV lost (thick lines) and converted to the energy of electrons (thin lines) at the distance  $r$  from the source. The injected proton spectrum is assumed power-law with an exponential cutoff  $J_p(E) = J_0 E^{-2} \exp(-E/E_0)$ , with  $E_0 = 3 \cdot 10^{20}$  eV.

Then the energy taken away by neutrinos is the difference between the energy lost by protons and the energy converted to electrons. As can be seen from Fig. 2, the protons with initial energies  $E > 10^{18}$  lose only 18% of their total energy after passing  $r = 100$  Mpc at the redshift  $z = 0.1$ , whereas at redshift  $z = 3$  the same protons lose 93% of the available energy already at  $r = 70$  Mpc, where the saturation begins. It can be explained by the fact that the cooling length of protons in the range  $E > 10^{18}$  eV do not exceed tens of Mpc at  $z = 3$ , while for redshifts  $z \ll 1$ , the protons have the cooling length of cosmological scales relative to pair production process. As the contribution of pair production increases, the share of energy lost by protons that goes to electrons increases from 74% at  $z = 0.1$  to 86% at  $z = 3$ .

The fraction of the initial energy of the protons with  $E > 10^{18}$  eV that can be converted to the electrons generated at photomeson processes depends strongly on the position of the cutoff energy. Left panel of Fig. 3 shows that the efficiency of extraction of proton energy and its transfer to this component of electrons grows with the redshift, and at  $z = 3$  all available for conversion energy is transferred at first 5 Mpc. The fraction of proton energy taken away by neutrinos in photomeson processes is 42% independently of redshift. Due to more energetic photons of CMBR, the threshold of photomeson interactions is shifted to lower energies that leads to the increase of extracted energy from 6% to 17% (see Fig. 3). However, as pair production begins to play a significant role at high redshifts the share of the electrons generated in photomeson processes is decreased, from 49% to 22% at the distance  $r = 100$  Mpc.

The importance of the shift of the reaction threshold on production of electrons becomes more obvious if the protons with energies close to threshold and higher are taken into account. The percentage of initial energy of protons with energies  $E > 10^{19}$  eV which is converted to the energy of electrons is presented in the right panel of Fig. 3. While at  $z = 0.1$  the production of electrons due to photomeson processes dominate at all distances smaller than 100 Mpc, at high redshifts the pair production prevails.

### 3. Gamma-ray source

Having the highest energy among secondaries, the electrons generated in photomeson processes emit almost all their energy via synchrotron radiation. Therefore, because of the shift of the threshold of photomeson interactions, the intensity of synchrotron gamma rays is increased with the redshift of the source. On the other hand, the reduction of cooling length of protons results in reduction of the apparent angular size of the region emitting synchrotron radiation, in addition to the diminution because of geometrical factor.

Fig. 4 shows spectral energy distribution of synchrotron gamma rays observed within different polar angle in the direction to the source of protons. The geometry of expanding Universe leads to more sophisticated dependence of apparent angular size on distance compared to the  $\sim 1/r$  dependence for the local Universe. It is useful to define a reference angle  $\theta_z^*$  which is equal to the angular size of the region with the radius  $r = 0.5$  Mpc located at the redshift  $z$ . Expressing the angles in units of corresponding reference angles, we can compare the regions located at different redshifts eliminating the geometrical factor. As expected, at large redshifts the reference angle increases with  $z$  (see Appendix A, Fig. A.1). In Fig. 4 for each redshift the fluxes are presented within three polar angles which differ from each other by factor of 3 and are expressed in the units of corresponding reference angle. The maximal angle indicated in plots is the polar angle within which the total flux is observed. Comparison of the maximal angles in units of reference angles shows a tendency of decreasing the angular size of the region of secondary synchrotron radiation with redshift, from  $9\theta_{0.1}^*$  to  $\theta_3^*/9$ .

The interaction of synchrotron gamma rays with extragalactic background light (EBL) leads to considerable attenuation of the flux. As it is seen from Fig. 4 the intergalactic absorption becomes substantial, depending on the distance to the source, from TeV energies down to tens of GeV energy range. For calculation of the absorption of gamma rays, the model of EBL developed in Franceschini et al. (2008) have been applied.

At high redshifts, the electrons from photomeson reactions are produced close to the acceleration sites of protons. In this case a considerable part of emitting electrons might be found in much stronger magnetic field compared to the average in-

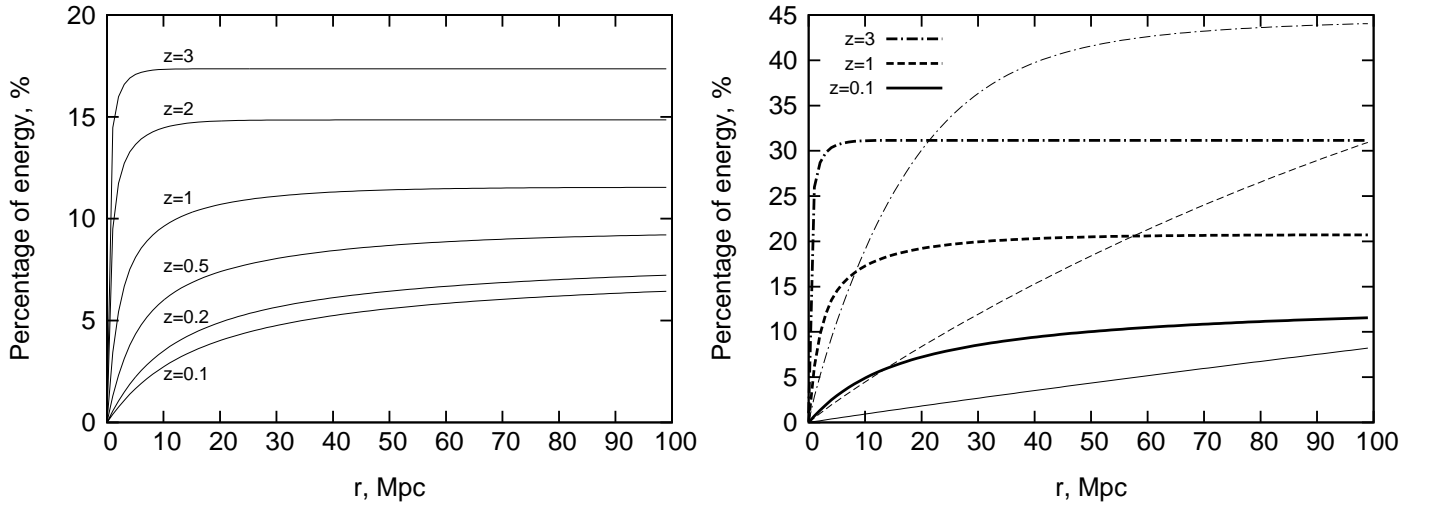


**Fig. 3.** Left panel: the fraction of the initial energy of protons with energy  $E > 10^{18}$  eV converted to the energy of electrons from *photomeson production* at distance  $r$  from the source. Right panel: the percentage of the initial energy of protons with energy  $E > 10^{19}$  eV converted to the energy of electrons from photomeson production (thick lines) and electrons from pair production (thin lines) at the distance  $r$  from the source.

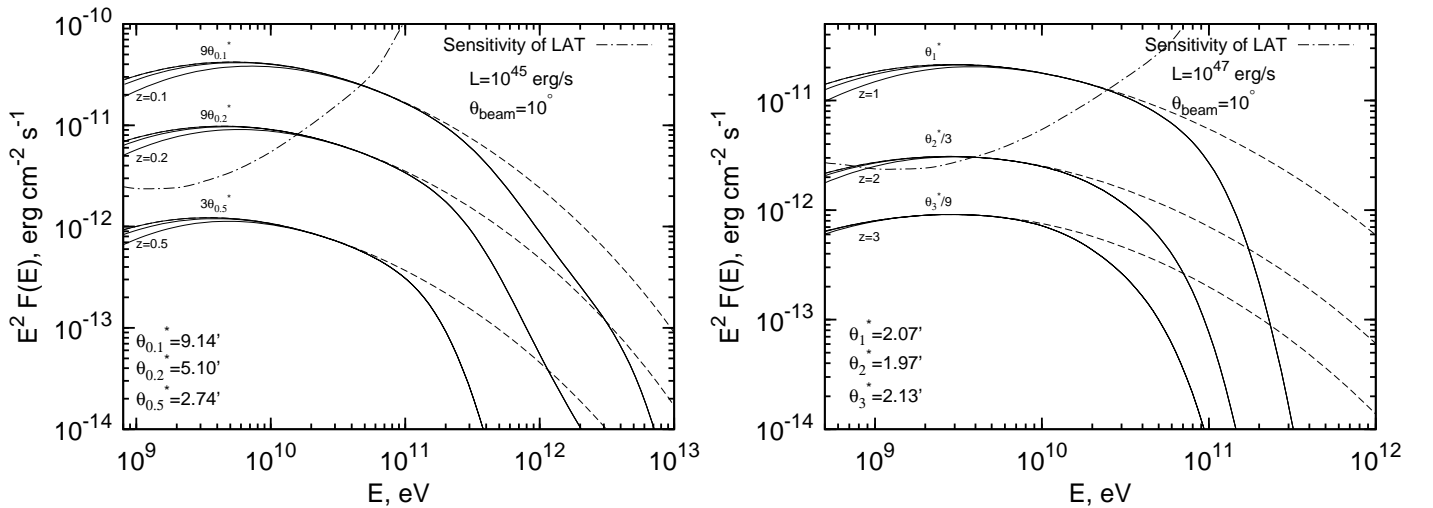


**Fig. 4.** Spectral energy distribution of gamma rays observed within different angles in the direction to the source with EBL absorption (thick lines) and without one (dashed lines) indicated for maximum angles.  $\theta_z^*$  is apparent angular size of the region with radius 0.5 Mpc from the distance with redshift  $z$ . The angles are specified in the units of corresponding  $\theta_z^*$  and differ from each other by factor of 3. The maximum angles for every redshift, the total power of injection of protons  $L$  and the beaming angle  $\theta_{beam}$  are indicated.

tergalactic field. The energy spectrum of synchrotron radiation of secondary electrons is shifted linearly with change of the strength of magnetic field to keep the ratio  $E_\gamma/B$  constant (see Aharonian et al. (2010)). Therefore the increase of the strength of magnetic field leads to the shift of radiation spectrum towards higher energies; if the radiation extends to TeV energies, the intergalactic absorption becomes quite violent; this results in the dissipation of almost the entire radiation. The absorbed gamma rays initiate cascades which contribute to the diffuse extragalactic background radiation.

Keeping in mind the sensitivity of instruments such as *Fermi*, the detection of the collimated synchrotron radiation from sources located at high redshifts is possible only in case of very powerful AGN. The anisotropic injection of UHE cosmic

rays allows to reduce the required power of source. Until deflection of protons is smaller than the angle of a jet, there is no difference between the spherically symmetric and anisotropic case. In both cases the observer will see identical pictures. For the given power of injection the existence of anisotropy with the opening angle  $\theta_{beam}$  of jet means the increase of the flux of gamma rays by the factor  $4/\theta_{beam}^2$  compared to the spherically symmetric case. The fluxes of synchrotron gamma rays in Fig. 4 are calculated for the case of  $\theta_{beam} = 10^\circ$ . The deflection of protons is smaller than this value of the opening angle while protons produce secondary particles. It is seen from Fig. 4 that at the power of proton injection  $L = 10^{45} - 10^{47}$  erg/s, the fluxes of gamma rays can exceed the sensitivity (minimum detectable fluxes) of *Fermi LAT* (Atwood et al. 2009) The resolution of the *Fermi LAT* varies in

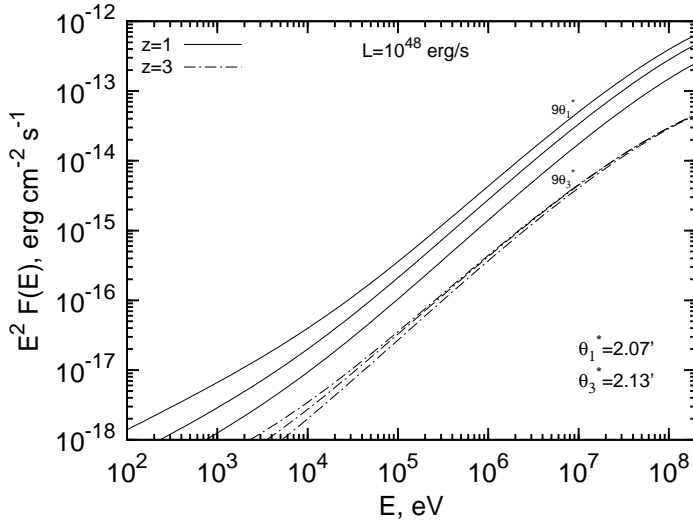


**Fig. 5.** Energy flux distribution of gamma- and X-rays observed within different angles in the direction of the source for the case of homogeneous magnetic field  $B = 1$  nG. Other parameters are the same as in previous figures.

dependence of photon energy from  $42'$  at  $E = 10^9$  eV to  $4.2'$  at  $E = 10^{11}$  eV (Atwood et al. 2009). Already for the source located at  $z = 0.2$  the angular size is  $46'$ , thus the source of gamma rays would be seen as extended one only if  $z < 0.2$ .

#### 4. X-ray emission

Protons lose part of their energy via pair production. The pair-produced electrons have lower energies compared to the electrons produced in photomeson processes and emit synchrotron radiation in the lower band of spectrum. At high redshifts the mean free path of protons relative to pair production process is decreased and generated electrons are located in more compact region. Moreover, the fraction of energy of protons converted to the secondary electron component is increased and reaches to 68% at  $z = 3$  (see Fig. 2, 3).

Synchrotron radiation for the strength of IGMF of  $B = 10^{-9}$  G and inverse Compton (IC) scattering give equal contribution to electron losses at energy  $E \approx 3 \cdot 10^{18}$  eV. At lower energies electrons lose their energy predominantly through IC scattering. Scattering is carried out at Klein-Nishina regime and almost all energy is transferred to photon. In turn the high energy photon produce electron-positron pair due to interaction with CMBR and most of the energy goes to one component of the pair which again suffer IC scattering. This process can be considered as alternation of the particle state with gradual reduction of energy. The electromagnetic cascade produces a huge halo of gamma rays with energy in GeV region. Region of synchrotron radiation is more compact, and electrons radiate it at the place of their generation. In spite of this the region is still quite extended as can be seen from angular distribution on Fig. 5. The flux of synchrotron radiation drops at low energies and becomes very small in X-ray region. The calculation of fluxes presented on Fig. 5 takes into account only homogeneous IGMF with strength  $B = 10^{-9}$  G. However, the strength of magnetic fields close to the accelerator can be much higher. To take this into account, we

consider the following spatial distribution for IGMF magnetic field:

$$B = B_{cl} \left( \frac{r_0}{r + r_0} \right)^3 + B_0, \quad (2)$$

where  $B_{cl} = 10^{-6}$  G is magnetic field in the cluster of galaxies with characteristic size of  $r_0 = 1$  Mpc,  $B_0 = 10^{-9}$  G is IGMF. Such a dependence of the magnetic field has been chosen to have a dipole behavior at large distances. For this case the energy and angular distributions of gamma- and X-rays are presented on left panels of Fig. 6 and 7. This magnetic field gives considerable increase of the fluxes of synchrotron radiation at low energies which is generated at small region close to the source and, therefore, has narrow angular distribution. Right panels shows that the contribution of electrons produced in pair production process (lower lines) is dominant in X-ray region, whereas gamma rays are generated predominantly by electrons produced in photomeson processes. Horizontal segments indicate sensitivity of *Chandra* (Lehmer et al. 2005; Romano et al. 2008) for corresponding maximum angles of observation. As can be seen the low energy part of X-rays (0.5–2 keV) is detectable for specified power of injection of protons, whereas the radiation at higher energies can be missing for sources located at high redshifts since *Chandra* is less sensitive in the range of energies 2 – 8 keV.

As follows from Fig. 6 and 7, the electrons produced in photomeson processes provide the main contribution to synchrotron gamma rays, although the most of energy lost by protons is contained in the low energy component of secondary electrons from the pair production process. The radiation of this component can be detected only in the case of a quite large,  $B_{cl} \approx 10^{-6}$  G magnetic field around the source. This can happen if the source is located inside a cluster of galaxies with a typical size of 1 Mpc. Nevertheless, even in the case of intensive pair production that takes place in cosmologically distant objects, only a small fraction of pairs is produced in the relatively compact region with a linear size of  $\sim 1$  Mpc (see Fig. 2); the most of energy of protons is converted to the energy of extended gamma ray halo.

#### 5. Summary

High energy gamma rays are unavoidably formed around the sources of UHE cosmic rays because of synchrotron radiation of secondary electrons produced at interactions of highest energy protons with the cosmic microwave background radiation. In our previous paper (Aharonian et al. (2010)) we have shown that even for relatively large intergalactic magnetic fields in the neighborhood of UHE cosmic ray accelerators,  $B \sim 10^{-7} - 10^{-9}$  G, these process lead to formation of high-energy point-like gamma-ray sources. Because of relatively weak gamma ray signals, the chances of detection of such sources are higher for objects located in the nearby Universe, namely at distances less than 100 Mpc. Since the efficiency of conversion of the proton energy to secondary gamma rays is dramatically reduced at protons energies  $E \leq 10^{20}$  eV, one may hope to detect gamma rays only from extreme objects accelerating protons to energies  $10^{20}$  eV and beyond. Given the fact that this requirement can be satisfied only in the case of unique combination of parameters, as well as the limited volume of the  $\leq 100$  Mpc region, realistically one can expect not a very large number of such sources. One can gain a lot if extends the study to cosmological distances. First of all, this allows to probe the most powerful objects in the Universe (e.g. quasars and AGNs) in which more favorable conditions can be formed for acceleration of protons to energies

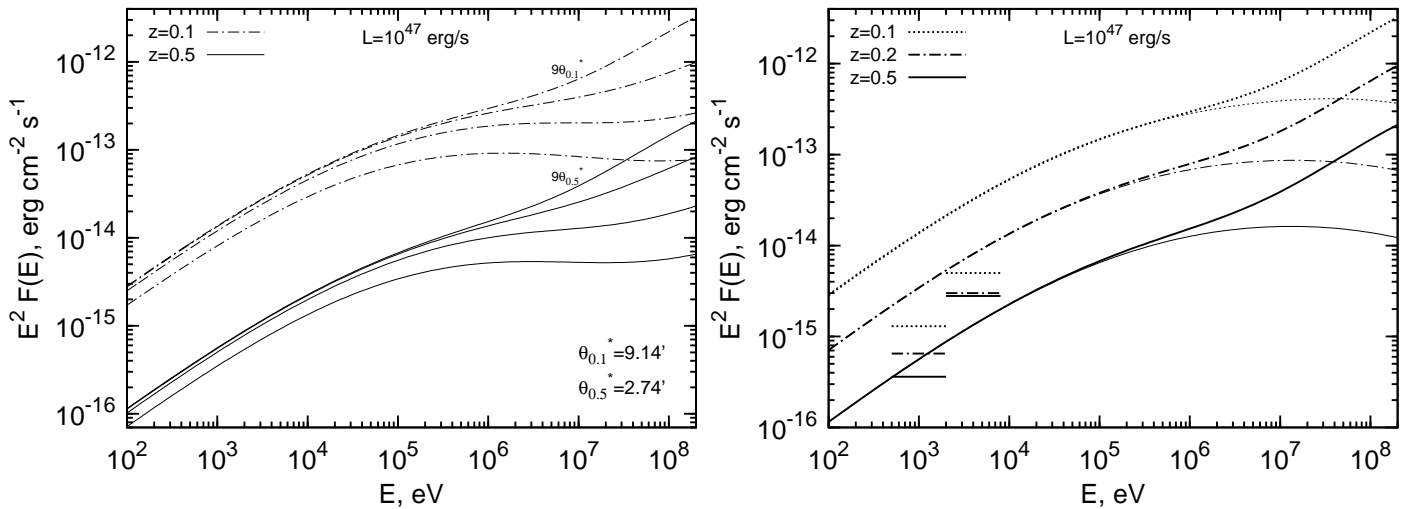


**Fig. 6.** Energy flux distribution of gamma- and X-rays observed within different angles in the direction of the source (left panel) and within maximum angle (right panel) for the case of two-band magnetic field. For the right panel, the total radiation from photomeson and pair production electrons (upper lines) and the radiation from pair production electrons (lower lines) are indicated. Horizontal segments present the *Chandra* sensitivity for the corresponding maximum angles of observation. The other parameters are the same as in previous figures.

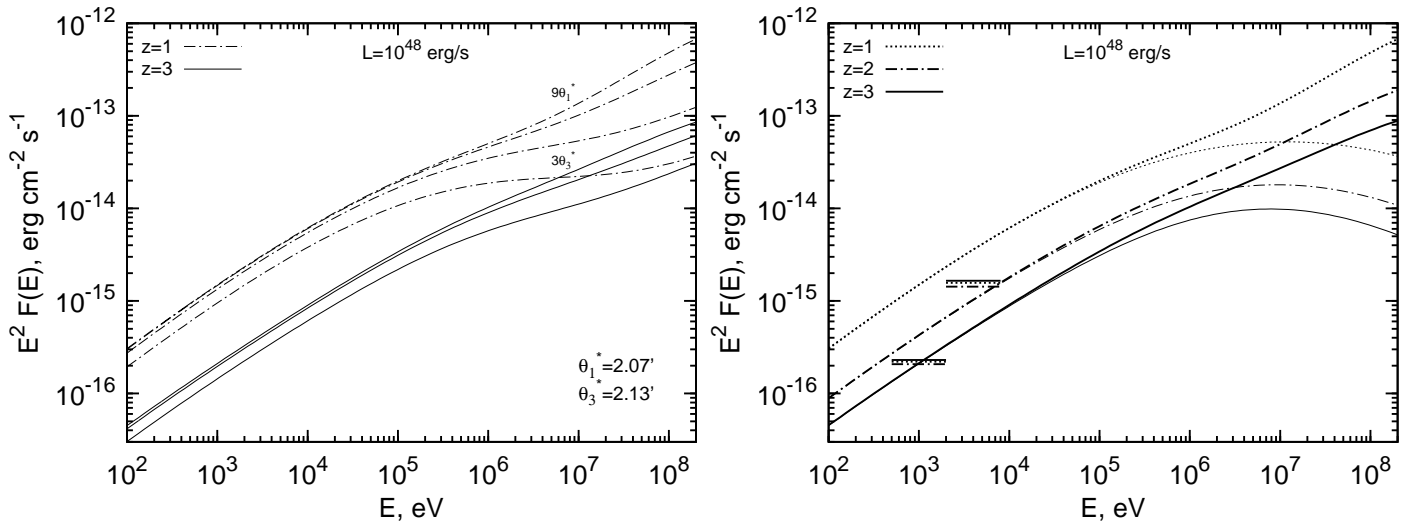


**Fig. 7.** The same as Fig. 6 but for  $z = 1, 2, 3$  and the total power of injection of protons  $L = 10^{48}$  erg/s.

$10^{20}$  eV. Secondly, because of higher temperature of the CMBR at cosmological epochs, i.e. because of denser and hotter relic photons, less energetic protons (with energy down to  $10^{19}$  eV) can lead to effective production of gamma rays. Given that the conditions of acceleration of protons to  $10^{19}$  eV in suspected cosmic accelerators are much relaxed as compared to the  $10^{20}$  eV extreme accelerators (see Aharonian et al. (2002)), we should expect dramatic increase of such gamma-ray sources. Another factor of enhancement of number of sources comes from the increase of the volume of the explored region to redshifts  $z \geq 3$ . An obvious caveat in this case is the decrease of gamma ray flux. However, this factor can be at least partly compensated by the huge power of objects in the remote Universe. Moreover, due to dramatic reduction of mean free paths of UHE protons at cosmological epochs  $z \geq 1$ , the conversion efficiency of proton energy to gamma rays is increased almost an order of magnitude, which makes these objects an extremely effective gamma-ray emitters.

Finally, since the secondary gamma-ray emission generally follows the direction of parent protons, the beamed cosmic accelerators like GRBs and blazars seem to be quite attractive targets for search of point-like but steady GeV gamma-ray emission from cosmologically distant objects.

### Appendix A: Angular size of sources at large redshifts and distribution function in the expanding Universe

If the radiation is generated on scales smaller than cosmological ones, the relevant processes can be considered as they take place in the conventional stationary Euclidean space. However, when radiation propagates over cosmological distances, the expansion of space should be taken into account. Based on the law of free motion of massless particles in expanding space, one can find the

distribution function of photons at the observation point. Then we need to convert the distribution function calculated in the reference frame with origin at the source to the reference frame of the observer (Kelner et al. (2011)). In the present paper the free propagation of photons is considered in the flat expanding Universe with parameters  $\Omega_\Lambda = 0.73$ ,  $\Omega_m = 0.27$  and  $H_0 = 71$  km/s Mpc.

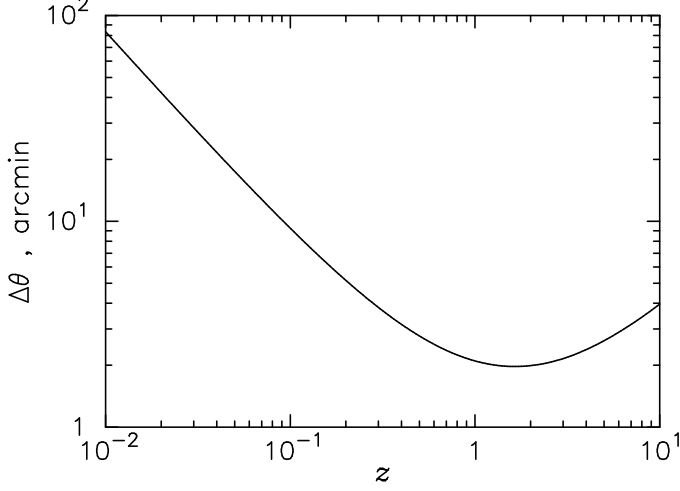


**Fig. A.1.** Angular size of the source with diameter  $D = 1$  Mpc located at different redshifts  $z$ .

We consider an isotropic gamma-ray source of radius  $R_*$  located at redshift  $z$ . Let us assume that photons escape this region with spherically symmetric distribution  $f_z(E, \theta)$ , where  $E$  is the energy of photon and  $\theta$  is the angle between photon momentum and radial direction at the escape point. Finally we assume that after the escape gamma rays propagate freely. In the case of small angles the distribution function  $f_0(z, E, \Omega(\theta))$  of gamma rays at the observation point integrated over the solid angle  $\Omega$  (with polar angle  $\theta$ ) can be expressed in the following form:

$$f_0(z, E, \Omega(\theta)) = 2\pi \left( \frac{\Theta_*}{1+z} \right)^2 \int_0^{\theta/\Theta_*} f_z(E(1+z), x) x dx, \quad (\text{A.1})$$

where

$$\Theta_* = \left( \frac{c}{H_0 R_* (1+z)} \int_0^z \frac{dz'}{\sqrt{\Omega_m (1+z')^3 + \Omega_\Lambda}} \right)^{-1}. \quad (\text{A.2})$$

The final result (A.1) differs from analogous one corresponding to the stationary space by the dependence on the redshift as well as by the nonlinear dependence of angular size on distance. The latter is determined by the parameter  $\Theta_*$  given by Eq. (A.2). The parameter  $\Delta\theta = 2\Theta_*$  has the meaning the angular size of the isotropically emitting source. In the case of anisotropic source, the angular size of radiation cannot be arbitrary large and is limited by  $\Delta\theta$ . In Fig. A.1 we show the angular size of the emission region with diameter  $D = 2R_* = 1$  Mpc. The parameter  $\Delta\theta$  has a minimum 1.95 arcmin at redshift  $z = 1.64$  when recession velocity equals to the speed of light  $c$  (Kelner et al. (2011)).

## References

Aharonian, F. A., Belyanin, A. A., Derishev, E. V., Kocharovskiy, V. V., & Kocharovskiy, V. V. 2002, Phys. Rev. D, 66, 023005

Aharonian, F. A., Kelner, S. R., & Prosekin, A. Y. 2010, Phys. Rev. D, 82, 043002  
 Atwood, W. B., Abdo, A. A., Ackermann, M., et al. 2009, ApJ, 697, 1071  
 Blasi, P. & Olinto, A. V. 1999, Phys. Rev. D, 59, 023001  
 Dolag, K., Grasso, D., Springel, V., & Tkachev, I. 2005, J. Cosmology Astropart. Phys., 1, 9  
 Essey, W., Kalashev, O., Kusenko, A., & Beacom, J. F. 2011, ApJ, 731, 51  
 Franceschini, A., Rodighiero, G., & Vaccari, M. 2008, A&A, 487, 837  
 Gabici, S. & Aharonian, F. A. 2005, Physical Review Letters, 95, 251102  
 Kelner, S. R., Prosekin, A. Y., & Aharonian. 2011, Phys. Rev. D, in preparation  
 Kotera, K., Allard, D., & Lemoine, M. 2011, A&A, 527, A54+  
 Lehmer, B. D., Brandt, W. N., Alexander, D. M., et al. 2005, ApJS, 161, 21  
 Romano, P., Campana, S., Mignani, R. P., et al. 2008, A&A, 488, 1221  
 Ryu, D., Kang, H., & Biermann, P. L. 1998, A&A, 335, 19  
 Sigl, G., Miniati, F., & Enßlin, T. A. 2004, Phys. Rev. D, 70, 043007  
 Taylor, A. M., Vovk, I., & Neronov, A. 2011, ArXiv e-prints